Raman: it's not just for noodles anymore

Mario Affatigato
Physics Department
Coe College

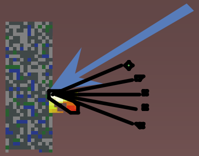

Outline - Lecture 1

- 1. Introduction
- 2. Theory
  - Role of polarizability; mathematical models
  - Depolarization ratio
  - Temperature correction
- 3. System instrumentation/common techniques
  - Components
  - FT-Raman
  - Raman microscopy

Outline - Lecture 2

- 4. Other Raman techniques
    - High pressure Raman spectroscopy
    - Surface enhanced Raman (SERS)
- 5. Vibrations and peak identification
- 6. Case studies
    - Silicates
    - Borates
    - Germanates
    - Other glass examples
- 7. References

1. Introduction

Introduction

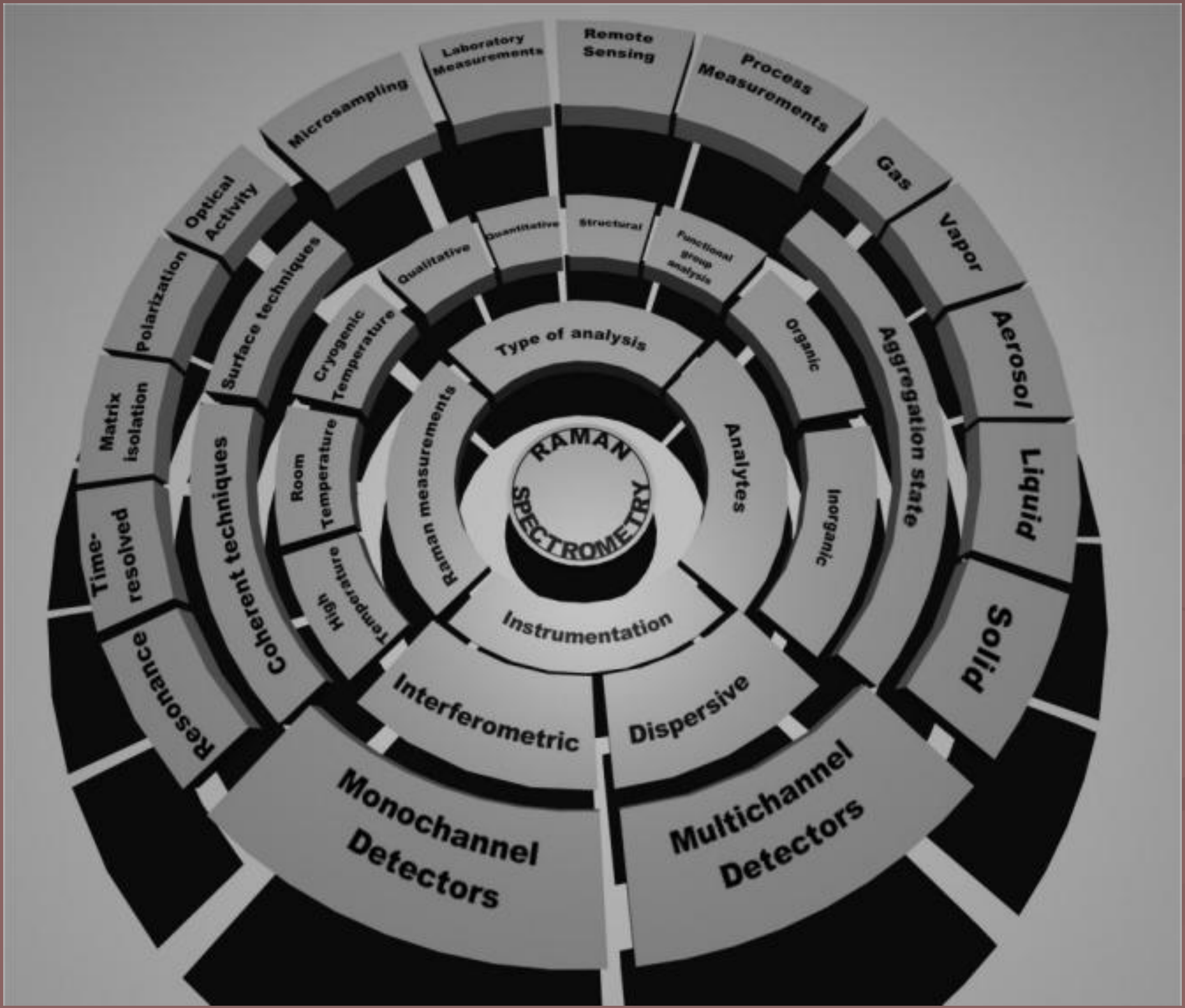

The graph on the left shows a good summary of the capabilities and kinds of Raman spectrometry. Just follow each quadrant and the different topics it includes.

(From: www.spectroscopynow.com/coi/cda/detail.cda?page=3&id=1882&type=EducationFeature&chId=6)

History

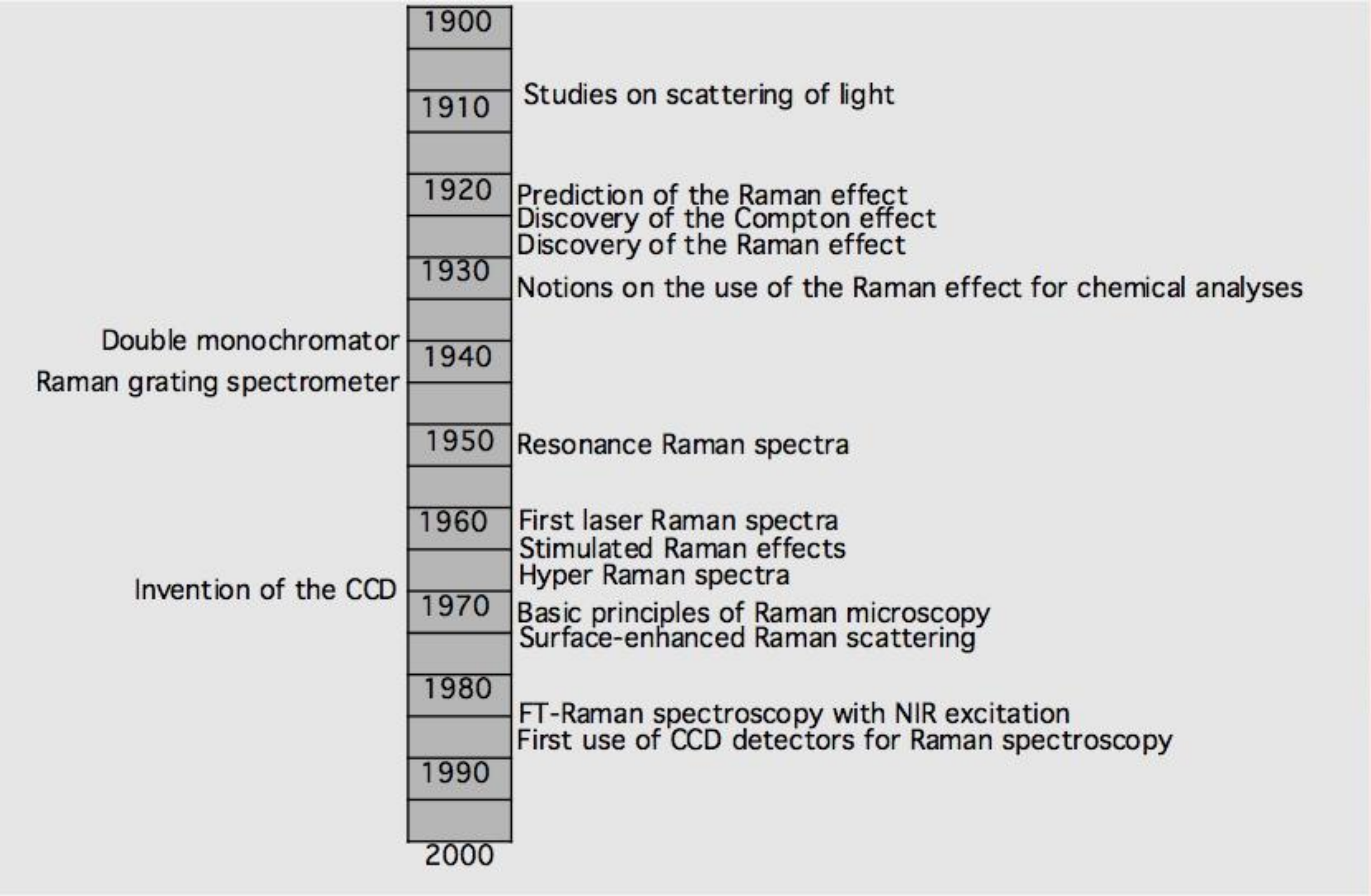

Studies on scattering of light

Prediction of the Raman effect
Discovery of the Compton effect
Discovery of the Raman effect

Notions on the use of the Raman effect for chemical analyses

Double monochromator
Raman grating spectrometer

Resonance Raman spectra

First laser Raman spectra
Stimulated Raman effects
Hyper Raman spectra

Invention of the CCD

Basic principles of Raman microscopy
Surface-enhanced Raman scattering

FT-Raman spectroscopy with NIR excitation
First use of CCD detectors for Raman spectroscopy

Advantages of Raman

- Selection rules allow for some vibrations (normally symmetric) to be seen only by Raman spectroscopy.
- Measurements of depolarization ratios yield information about molecular symmetry.
- Only a small sample area is needed (laser spot).
- Water is a weak Raman scatterer, allowing for the use of aqueous solutions. Can also sample through glass container walls.
- The region 4000 cm^{-1} to 50 cm^{-1} can be covered in a single scan without changing gratings, splitters, detectors, etc.

Disadvantages of Raman

- Laser source is needed, which can cause local heating/decomposition.
- Can cause fluorescence.
- More difficult to obtain rotational and ro-vibrational spectra with high resolution
- Way more expensive: 150-200 k$ vs. 40-60 k$ for FTIR.

Raman virtual states

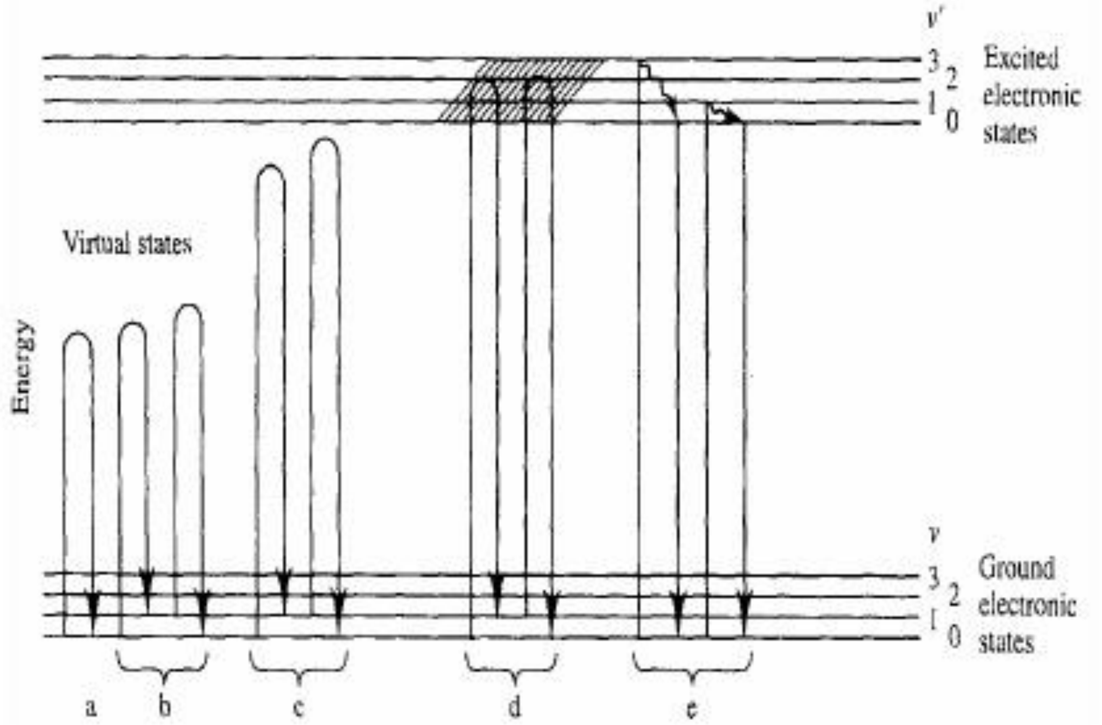

Figure 1 : Mechanisms of various light-scattering processes. (a) Rayleigh, (b) non-resonance Raman, (c) pre-resonance Raman, (d) resonance Raman and (e) resonance fluorescence

Stokes/Anti-Stokes

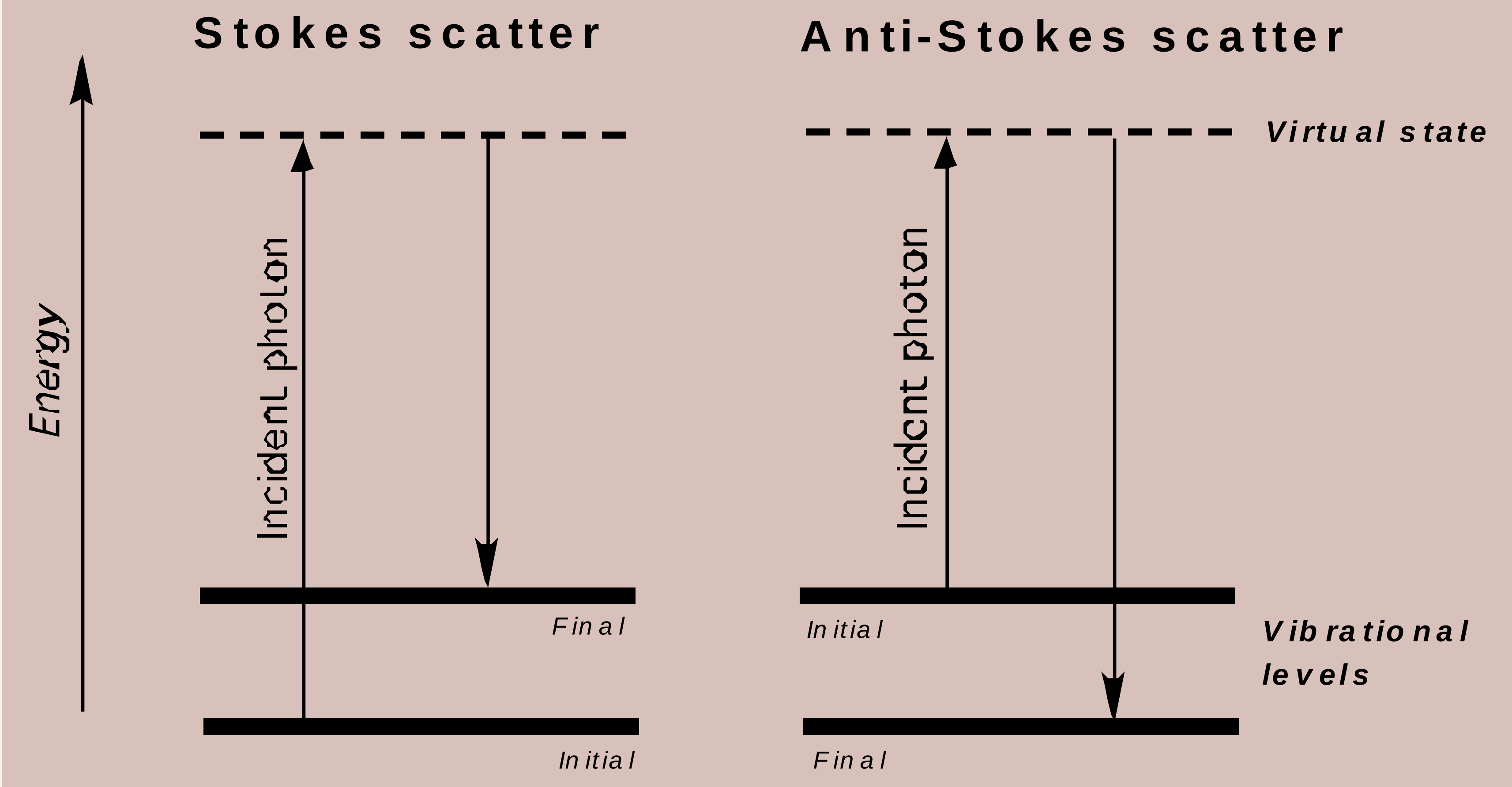

Note that the transitions (scattering) take 10^{-14} seconds or le

Stokes and anti-Stokes

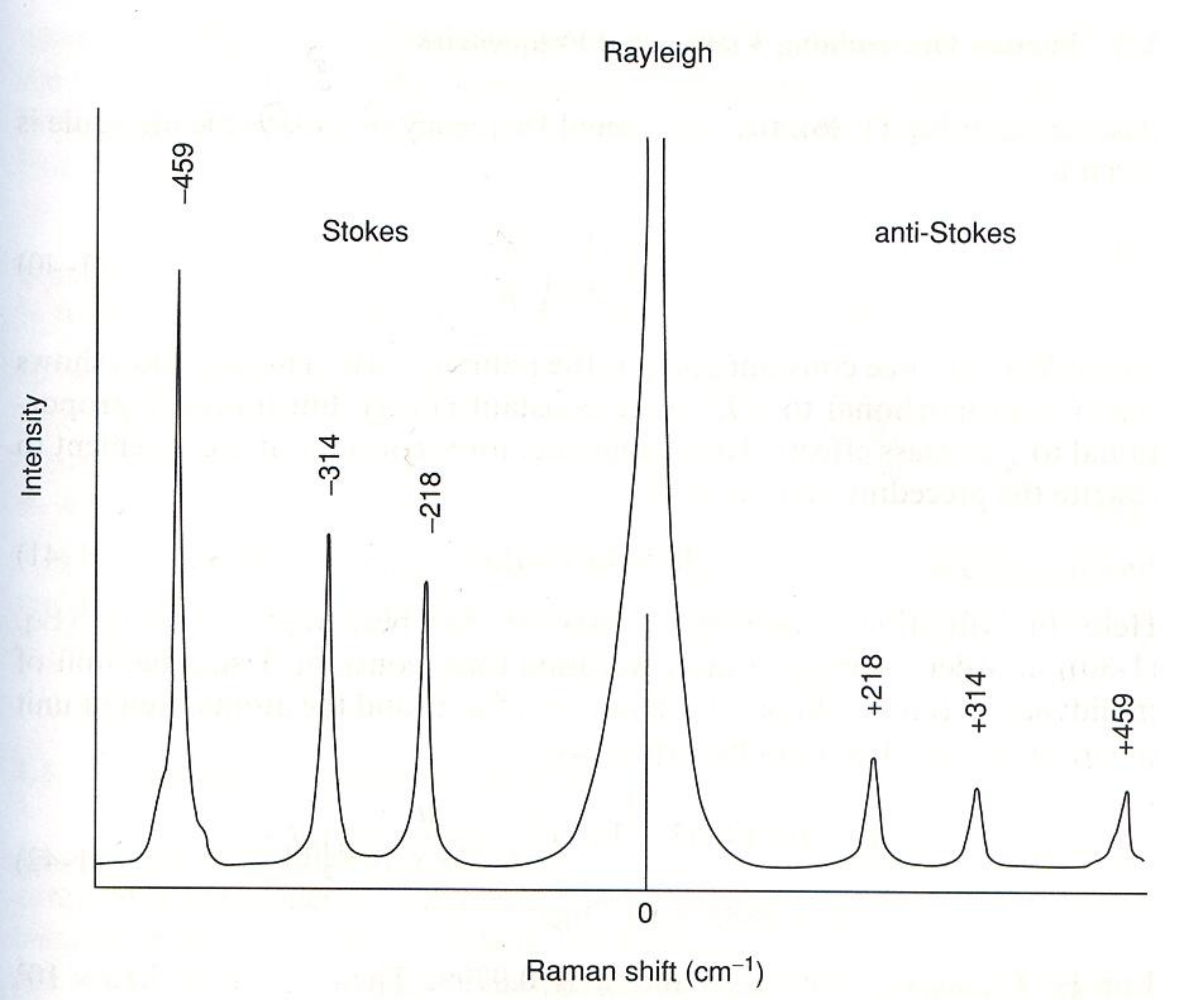

Figure 1-9 Raman spectrum of CCl_4 (488.0 nm excitation).

As you can see, the Stokes peaks correspond to lower photon frequencies and lower energies. The anti-Stokes side is symmetric but corresponds to higher frequencies and energies. The Stokes lines are stronger because the population of molecules at $\nu=0$ is much larger than at $\nu=1$ by the Maxwell-Boltzmann distribution law.

2. Theory

Some classical Raman theory

Let light $E = E_0 Cos\ 2\pi\nu_0 t$ shine on a diatomic molecule. The induced dipole moment is

$P = \alpha E = \alpha E_0 Cos\ 2\pi\nu_0 t$. Here α is the polarizability of the molecule.

If the molecule is vibrating with frequency ν_m then the displacement (nuclear) is given by

$q = q_0 Cos\ 2\pi\nu_m t$. For small amplitudes, we consider α as a linear function of q, so

$\alpha = \alpha_0 + \left(\frac{\partial\alpha}{\partial q}\right)_0 q_0 + \ldots$ Then the combined equations yield

$$P = \alpha E_0 Cos\ 2\pi\nu_0 t = \alpha_0 Cos\ 2\pi\nu_0 t + \left(\frac{\partial\alpha}{\partial q}\right)_0 qE_0 Cos\ 2\pi\nu_0 t =$$

$$\alpha_0 Cos\ 2\pi\nu_0 t + \left(\frac{\partial\alpha}{\partial q}\right)_0 q_0 E_0 Cos\ 2\pi\nu_0 t \bullet Cos\ 2\pi\nu_m t =$$

$$\alpha_0 Cos\ 2\pi\nu_0 t + \frac{1}{2}\left(\frac{\partial\alpha}{\partial q}\right)_0 q_0 E_0 [Cos\ \{2\pi(\nu_0 + \nu_m)t\} + Cos\ \{2\pi(\nu_0 - \nu_m)t\}]$$

Some classical Raman theory

Let light $E = E_0 Cos\ 2\pi\nu_0 t$ shine on a diatomic molecule. The induced dipole moment is

$P = \alpha E = \alpha E_0 Cos\ 2\pi\nu_0 t$. Here α is the polarizability of the molecule.

If the molecule is vibrating with frequency ν_m then the displacement (nuclear) is given by

$q = q_0 Cos\ 2\pi\nu_m t$. For small amplitudes, we consider α as a linear function of q, so

$\alpha = \alpha_0 + \left(\frac{\partial\alpha}{\partial q}\right)_0 q_0 + \ldots$ Then the combined equations yield

$$P = \alpha E_0 Cos\ 2\pi\nu_0 t = \alpha_0 Cos\ 2\pi\nu_0 t + \left(\frac{\partial\alpha}{\partial q}\right)_0 q E_0 Cos\ 2\pi\nu_0 t =$$

$$\alpha_0 Cos\ 2\pi\nu_0 t + \left(\frac{\partial\alpha}{\partial q}\right)_0 q_0 E_0 Cos\ 2\pi\nu_0 t \bullet Cos\ 2\pi\nu_m t =$$

$$\alpha_0 Cos\ 2\pi\nu_0 t + \frac{1}{2}\left(\frac{\partial\alpha}{\partial q}\right)_0 q_0 E_0 [Cos\ \{2\pi(\nu_0 + \nu_m)t\} + Cos\ \{2\pi(\nu_0 - \nu_m)t\}]$$

Some classical Raman theory

Let light $E = E_0 Cos\ 2\pi\nu_0 t$ shine on a diatomic molecule. The induced dipole moment is

$\boxed{P = \alpha E} = \alpha E_0 Cos\ 2\pi\nu_0 t$. Here α is the polarizability of the molecule.

If the molecule is vibrating with frequency ν_m then the displacement (nuclear) is given by

$q = q_0 Cos\ 2\pi\nu_m t$. For small amplitudes, we consider α as a linear function of q, so

$\alpha = \alpha_0 + \left(\frac{\partial\alpha}{\partial q}\right)_0 q_0 + \dots$ Then the combined equations yield

$$P = \alpha E_0 Cos\ 2\pi\nu_0 t = \alpha_0 Cos\ 2\pi\nu_0 t + \left(\frac{\partial\alpha}{\partial q}\right)_0 q E_0 Cos\ 2\pi\nu_0 t =$$

$$\alpha_0 Cos\ 2\pi\nu_0 t + \left(\frac{\partial\alpha}{\partial q}\right)_0 q_0 E_0 Cos\ 2\pi\nu_0 t \bullet Cos\ 2\pi\nu_m t =$$

Anti-Stokes Stokes

$$\alpha_0 Cos\ 2\pi\nu_0 t + \frac{1}{2}\left(\frac{\partial\alpha}{\partial q}\right)_0 q_0 E_0 [Cos\ \{2\pi(\boxed{\nu_0 + \nu_m})t\} + Cos\ \{2\pi(\boxed{\nu_0 - \nu_m})t\}]$$

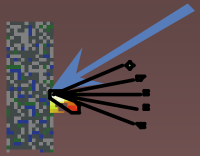

More math

In actual molecules, the nice linear relationship does not hold since both P and E are vectors. Then the equation must be written as

$$\begin{bmatrix} P_x \\ P_y \\ P_z \end{bmatrix} = \begin{bmatrix} \alpha_{xx} & \alpha_{xy} & \alpha_{xz} \\ \alpha_{yx} & \alpha_{yy} & \alpha_{yz} \\ \alpha_{zx} & \alpha_{zy} & \alpha_{zz} \end{bmatrix} \begin{bmatrix} E_x \\ E_y \\ E_z \end{bmatrix}$$

The matrix is called the *polarizability tensor*. We can plot α_i (α in the i direction) in all directions we get a 3D surface. Conventionally we plot $1/\sqrt{\alpha_i}$ instead, and get a *polarizability ellipsoid*.

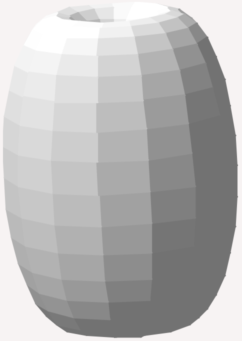

CO_2 Polarizability ellipsoids

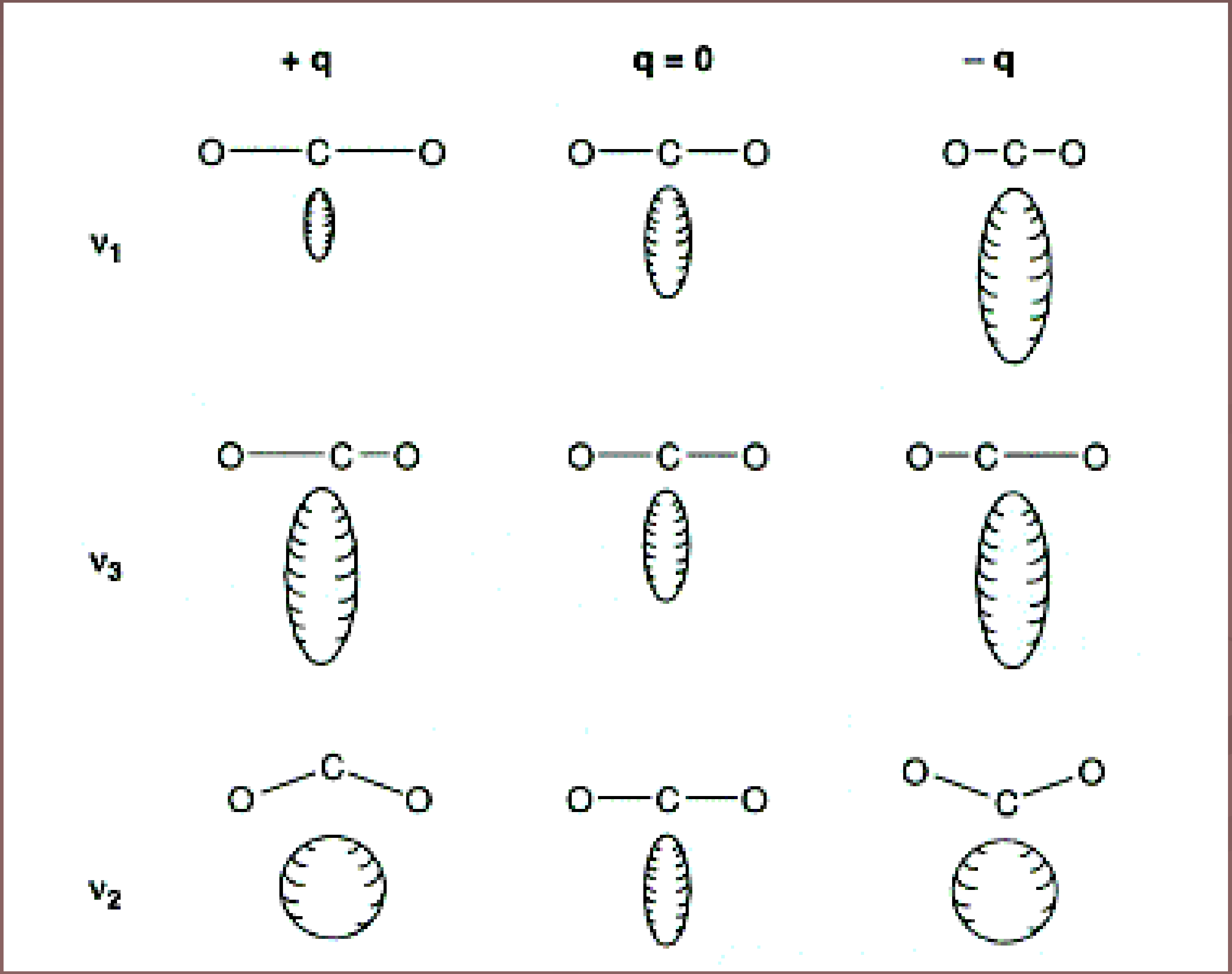

Raman active

IR active

IR active

Scattering

- Classically, the observed intensity of Raman scattering is proportional to
  - $I_R = \mu(\nu_0 \pm \nu_j)^4 \alpha_j^2 Q_j^2$

where ν_0 is the laser light frequency, ν_j is the frequency of the jth mode, Q_j the displacement, and α is the polarizability of that mode. **Note the dependence on the fourth power of the laser light**, typical for dipole scattering.

Depolarization ratio

- The depolarization ratio is defined as the ratio of the light scattered at 90 degrees that is perpendicular (I_y) to the light that is parallel ($I_{||}$) with respect to the incident light.
- The incident laser light is already polarized. But the scrambler is required because monochromator gratings show different efficiencies for the different polarizations.

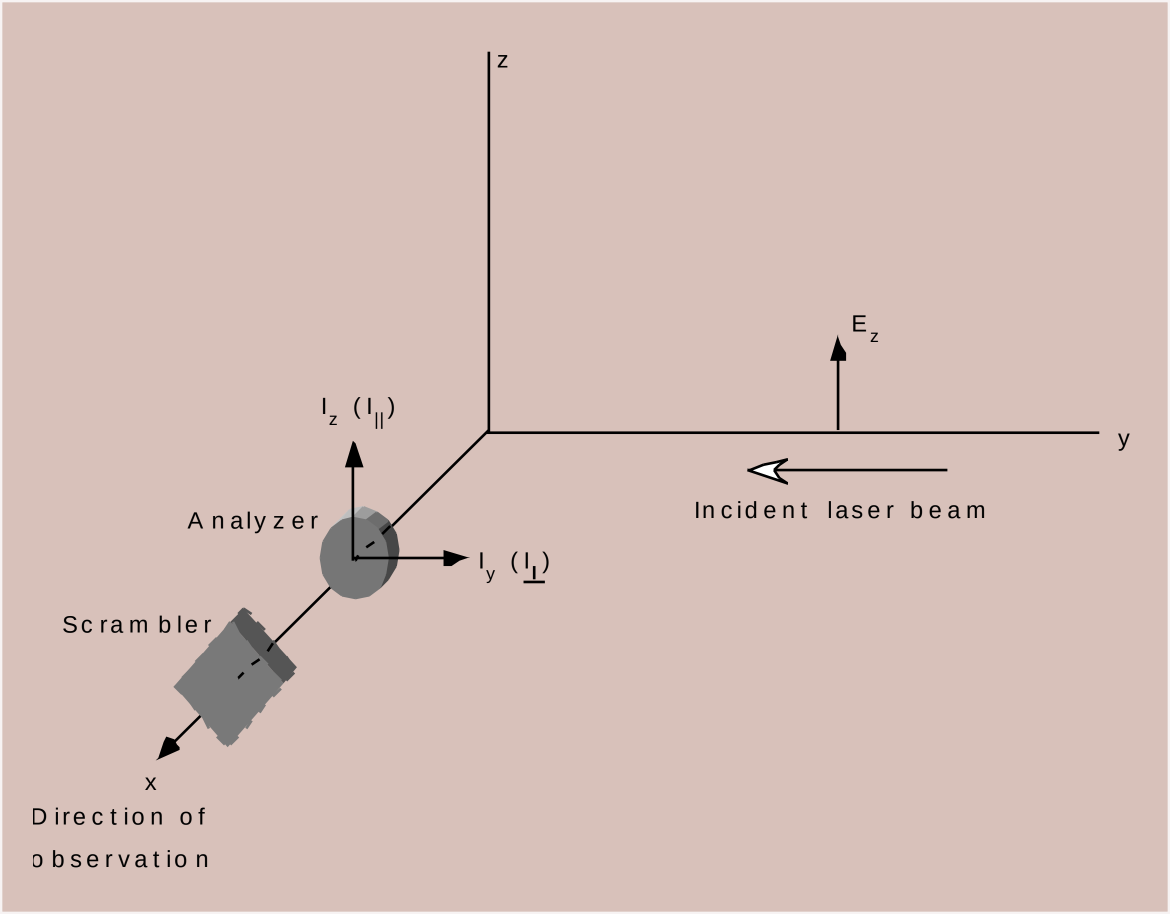

(Original diagram from J.R. Ferraro, in References)

Depolarization ratio

Since the ratio is defined as $\rho_p = \frac{I_y}{I_z}$, and it can be shown that this is related to the polarizability matrix by

$$\rho_p = \frac{3g^s + 5g^a}{10g^0 + 4g^s}, \quad \text{where} \quad \begin{aligned} g^0 &= \frac{1}{3}\left(\alpha_{xx} + \alpha_{yy} + \alpha_{zz}\right)^2 \\ g^s &= \frac{1}{3}\left[(\alpha_{xx} - \alpha_{yy})^2 + (\alpha_{yy} - \alpha_{zz})^2 + (\alpha_{zz} - \alpha_{xx})^2\right] \\ &+ \frac{1}{2}\left[(\alpha_{xy} + \alpha_{yx})^2 + (\alpha_{yz} + \alpha_{zy})^2 + (\alpha_{xz} + \alpha_{zx})^2\right] \\ g^a &= \frac{1}{2}\left[(\alpha_{xy} - \alpha_{yx})^2 + (\alpha_{xz} - \alpha_{zx})^2 + (\alpha_{yz} - \alpha_{zy})^2\right] \end{aligned}$$

In normal Raman scattering, $g^a = 0$ from symmetry. For totally symmetric vibration, we then get $0 \leq \rho_p < \frac{3}{4}$, while for non-totally symmetric vibration $\rho_p = \frac{3}{4}$

Depolarization ratio

Since the ratio is defined as $\rho_p = \frac{I_y}{I_z}$, and it can be shown that this is related to the polarizability matrix by

$$\rho_p = \frac{3g^s + 5g^a}{10g^0 + 4g^s}, \quad \text{where}$$

$$g^0 = \frac{1}{3}\left(\alpha_{xx} + \alpha_{yy} + \alpha_{zz}\right)^2$$

$$g^s = \frac{1}{3}\left[(\alpha_{xx} - \alpha_{yy})^2 + (\alpha_{yy} - \alpha_{zz})^2 + (\alpha_{zz} - \alpha_{xx})^2\right]$$

$$+ \frac{1}{2}\left[(\alpha_{xy} + \alpha_{yx})^2 + (\alpha_{yz} + \alpha_{zy})^2 + (\alpha_{xz} + \alpha_{zx})^2\right]$$

$$g^a = \frac{1}{2}\left[(\alpha_{xy} - \alpha_{yx})^2 + (\alpha_{xz} - \alpha_{zx})^2 + (\alpha_{yz} - \alpha_{zy})^2\right]$$

In normal Raman scattering, $g^a = 0$ from symmetry. For totally symmetric vibration, we then get $\boxed{0 \le \rho_p < \frac{3}{4}}$, while for non-totally symmetric vibration $\boxed{\rho_p = \frac{3}{4}}$

Depolarization of CCl_4

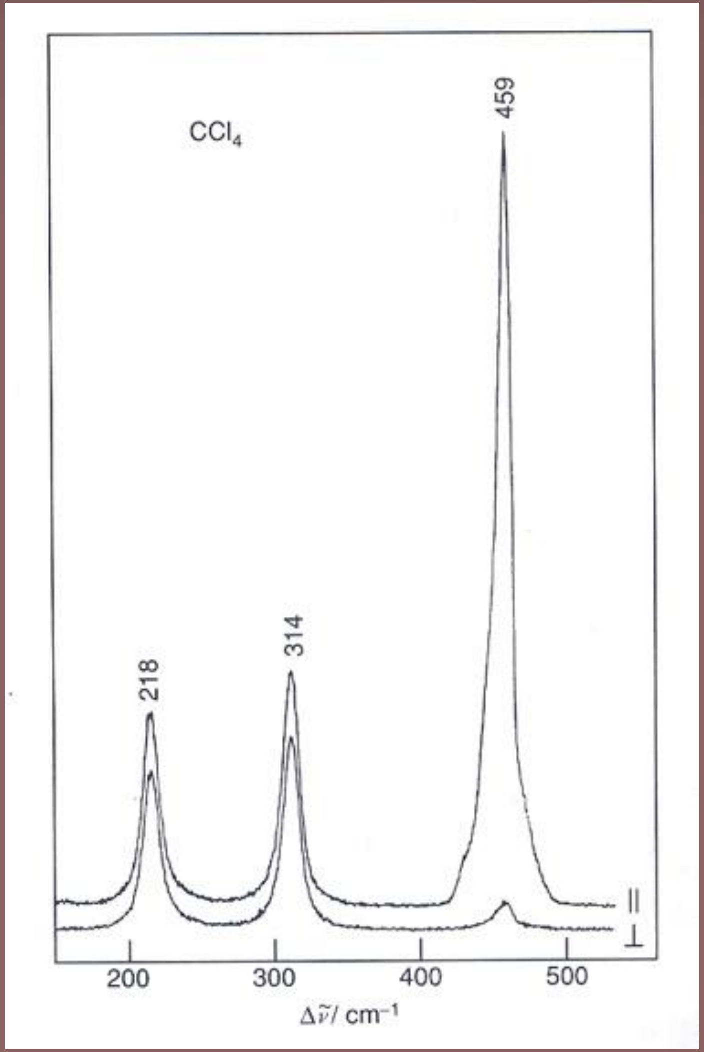

- In the spectrum on the left you see the totally symmetric vibrations of CCl_4 (459 cm^{-1}) and the non-totally symmetric modes (314 and 218 cm^{-1}), taken in a 90° scattering geometry. The values of ρ_p were 0.02 for the first case (459 cm^{-1}; note ratio of peaks), and 0.75 for the other two peaks, as expected.
- Though usually done with liquids and gases, depolarization measurements can be done in solids by suspending them in a material with a similar index.

CCl$_4$ modes and Raman

QuickTime™ and a
Animation decompressor
are needed to see this picture.

- Animation from

http://fy.chalmers.se/~brodin/MolecularMotions/CCl4molecule.html

Temperature correction

- The thermal population factor can mask peaks or bands in the low-frequency region of the spectrum. The corrected (reduced) Raman intensity can be calculated from

$$I_{reduced} = \frac{I_{observed}}{Exp\left[-\frac{\hbar\omega}{kT}\right] + 1}$$

- This needs to be done before any peak assignments are made

Temperature correction

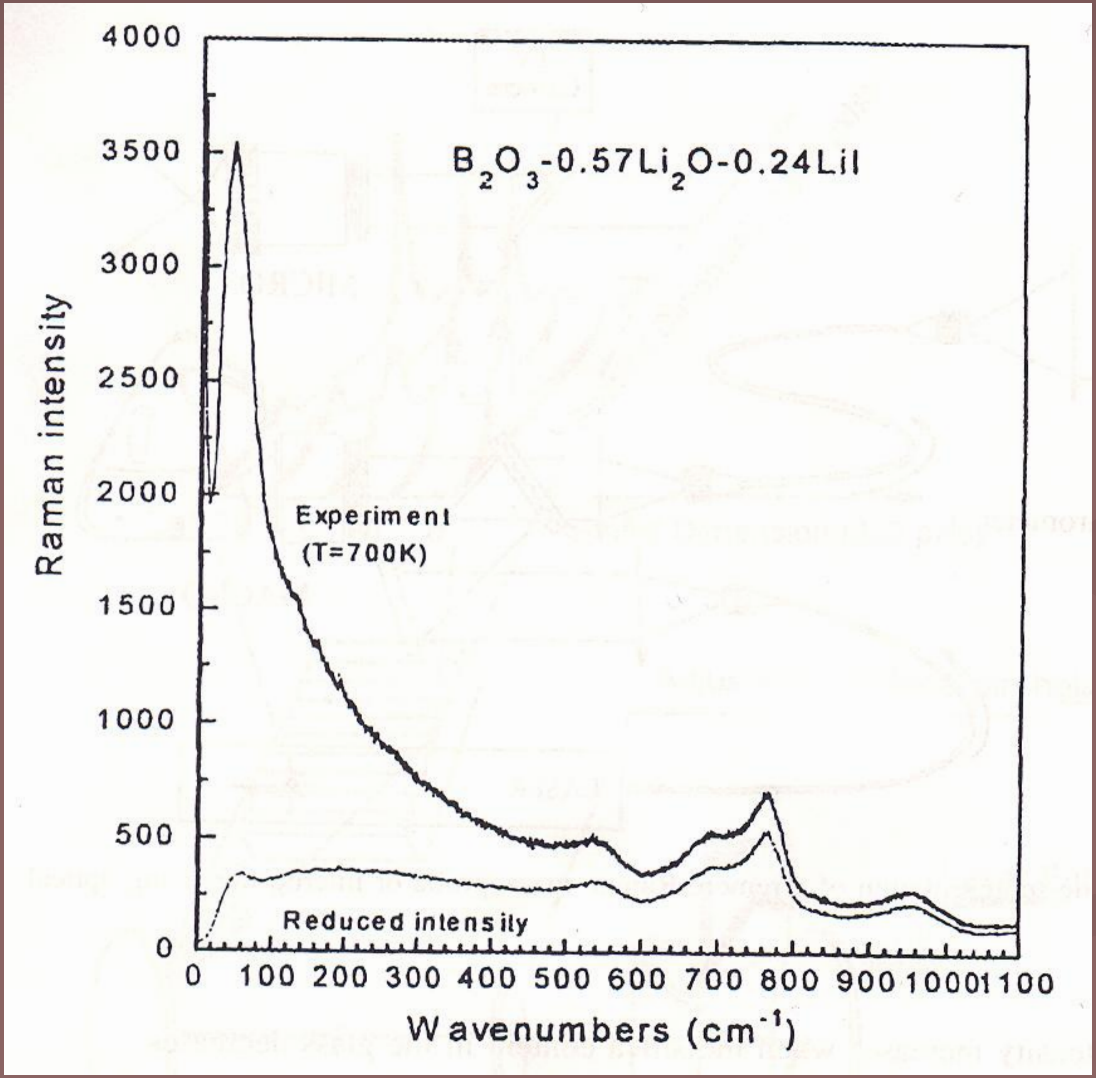

- The effect of the temperature correction can be seen at left, where the most dramatic change occurs at low wavenumbers.

3. System components and common techniques

Simplified Raman spectrometer layout

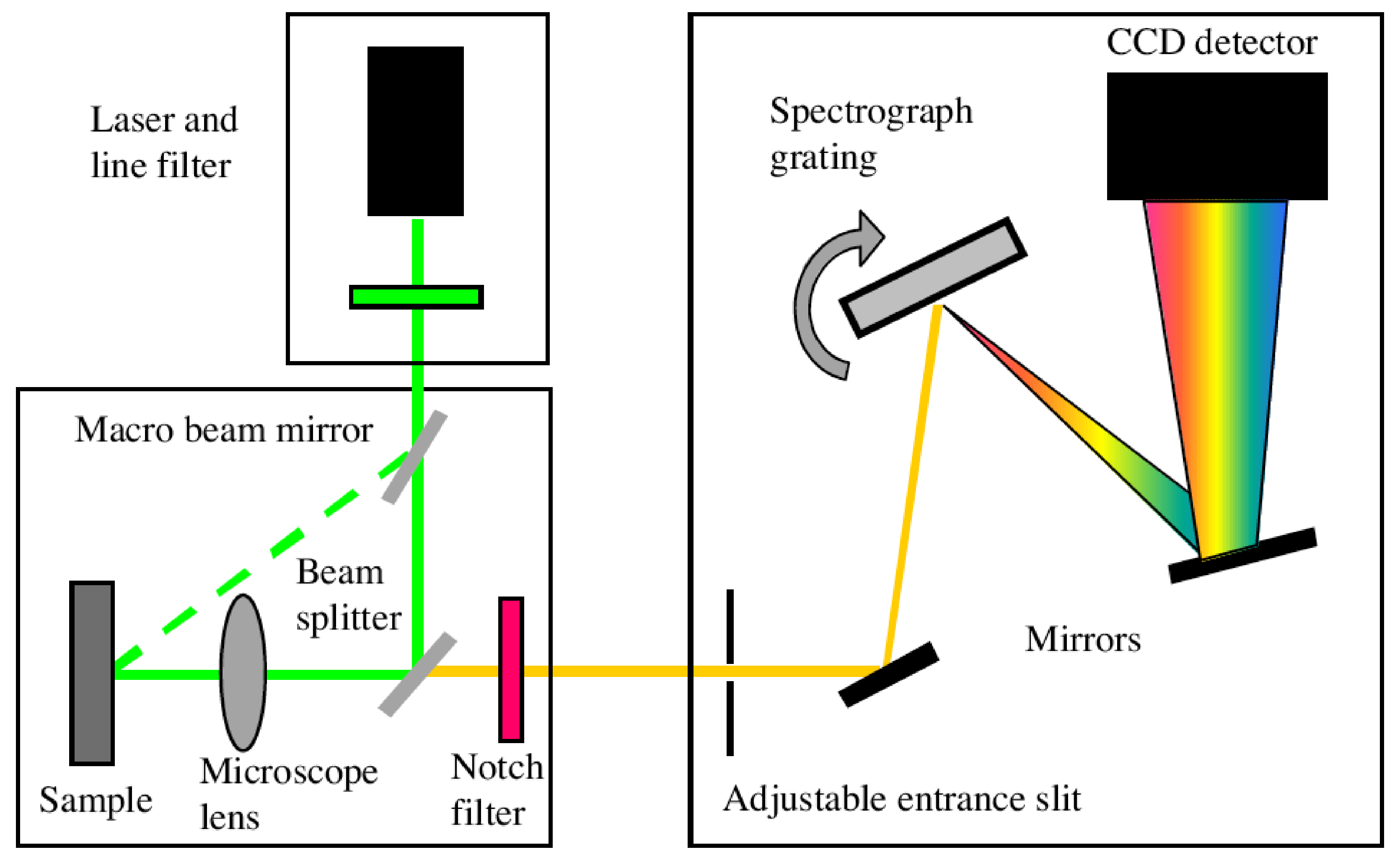

Lasers

For a long time the most common laser for a Raman system was the Ar:ion laser, which provided multiple lines (wavelengths). Cost was significant, however, as were maintenance costs. Nowadays the selection is much greater: Gas Ion, HeNe, DPSS 532 nm, Solid-state visible lasers, NIR Diode, High power fibre linked, UV lasers

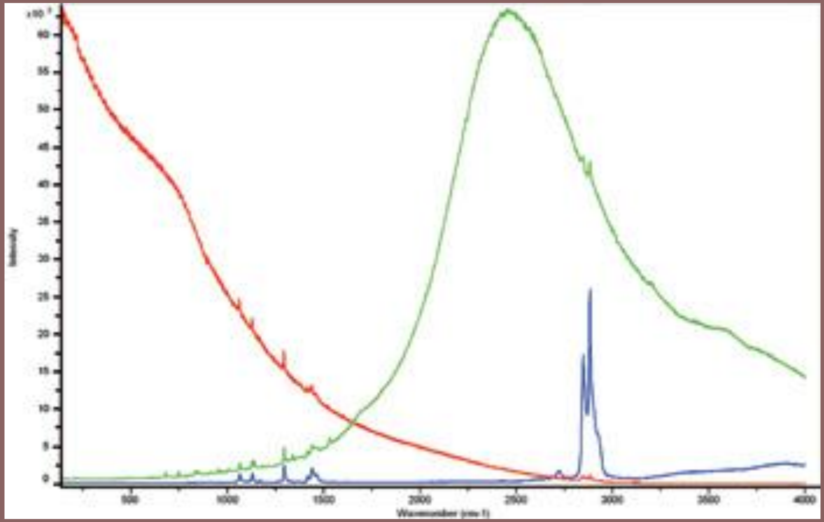

The key is what laser can minimize the fluorescence signal of the sample. On the left we see a sample irradiated with green light (too fluorescent); red light (still too much), and NIR (785 nm; just right)

Exercise

- Which of the following lasers would yield best results when measuring weak Raman signals, and approximately by how much?
  - Green argon line (514.5 nm) *vs.* blue argon line (488 nm):
  - Nd:YAG fundamental (1064 nm) *vs.* diode laser (785 nm):

EXERCISE

- Which of the following lasers would yield best results when measuring weak Raman signals, and approximately by how much?
  - Green argon line (514.5 nm) *vs.* blue argon line (488 nm):

$$\frac{514.5^{4}}{488^{4}} = 1.24$$

*

  - Nd:YAG fundamental (1064 nm) *vs.* diode laser (785 nm):

$$\frac{1064^{4}}{785^{4}} = 3.37$$

*

Spectrographs

- The most common spetrograph arrangement is the Czerny-Turner, shown on the right. The mirrors are used as collimators, and the turret contains planar reflective gratings.

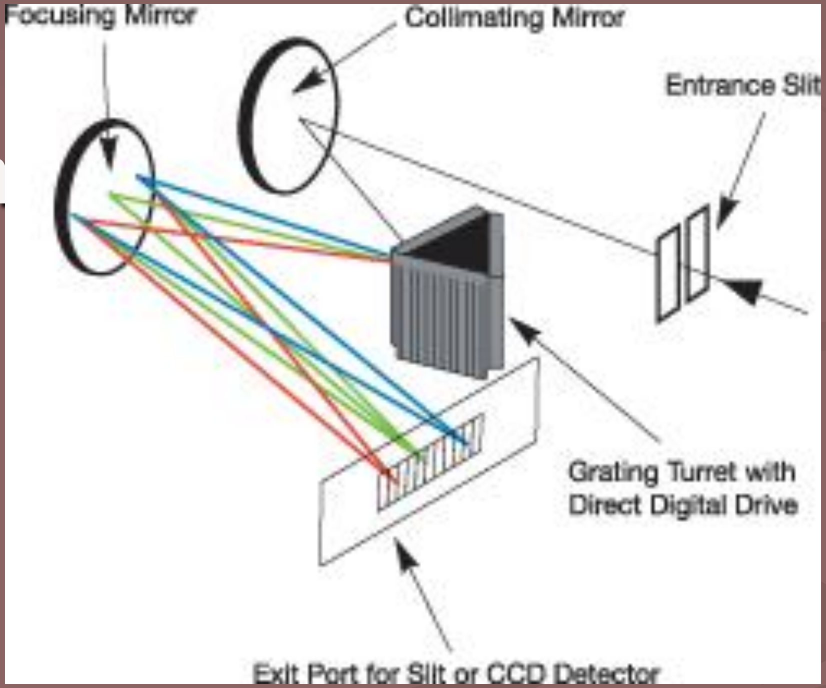

Spectrographs

- For higher resolution and rejection of unwanted (read Rayleigh) wavelengths, one can use a double or triple monochromator. This adds to the price and diminishes the overall light signal.

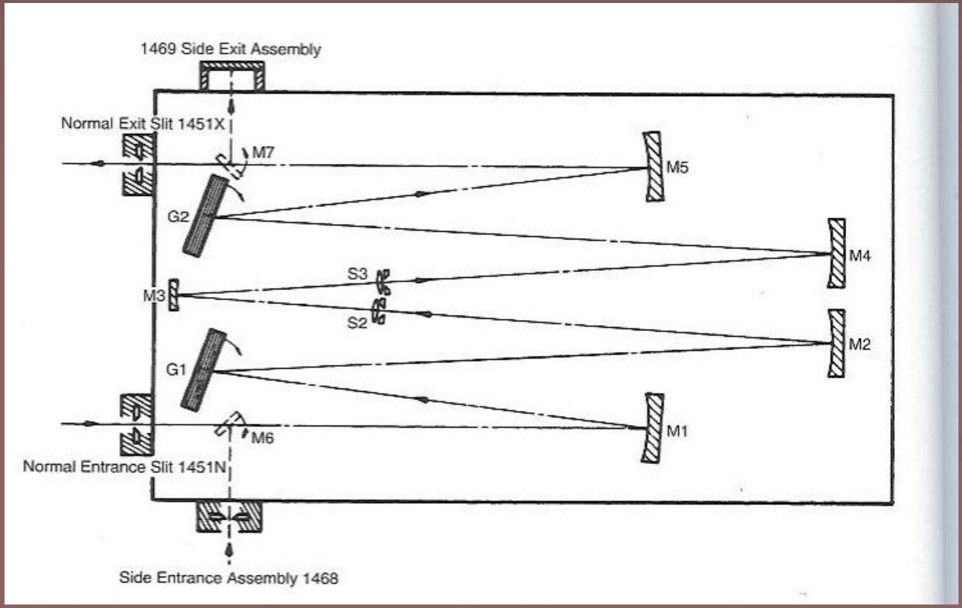

CCD Detectors

- Most of the current dispersive Raman set-ups are now equipped with multichannel two-dimensional CCD detectors. The main advantages of these detectors are the high quantum efficiency, the extremely low level of thermal noise (when effectively cooled), low read noise and the large spectral range available. Many CCD chips exist, but one of the most common spectroscopy sensor formats is the 1024 x 256 pixel array.

FT-Raman

Advantages and disadvantages of FT-Raman

- Use of NIR lasers greatly reduces fluorescence problem
- Relatively inexpensive (less so lately!)
- High resolution, high throughput
- Collects Stokes and Anti-Stokes simultaneously
- Can be attached to an IR instrument

But…

- Black body emissions at higher temp swamp Raman
- Lower scattering intensity due to use of NIR (ν^4 effect)
- Absorptions in the NIR
- Slow (tens of minutes in some systems)

Michelson interferometer

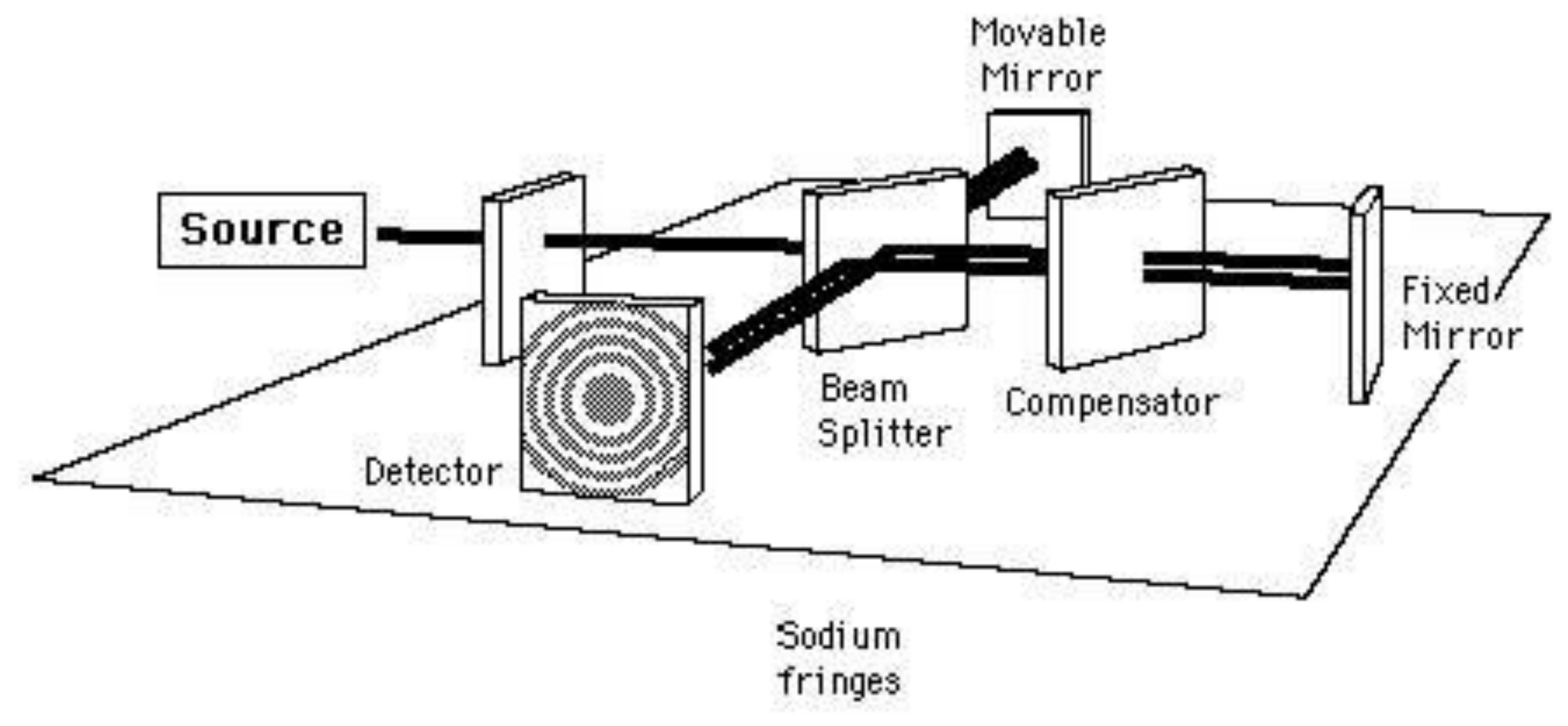

3D view

FT-Raman schematic

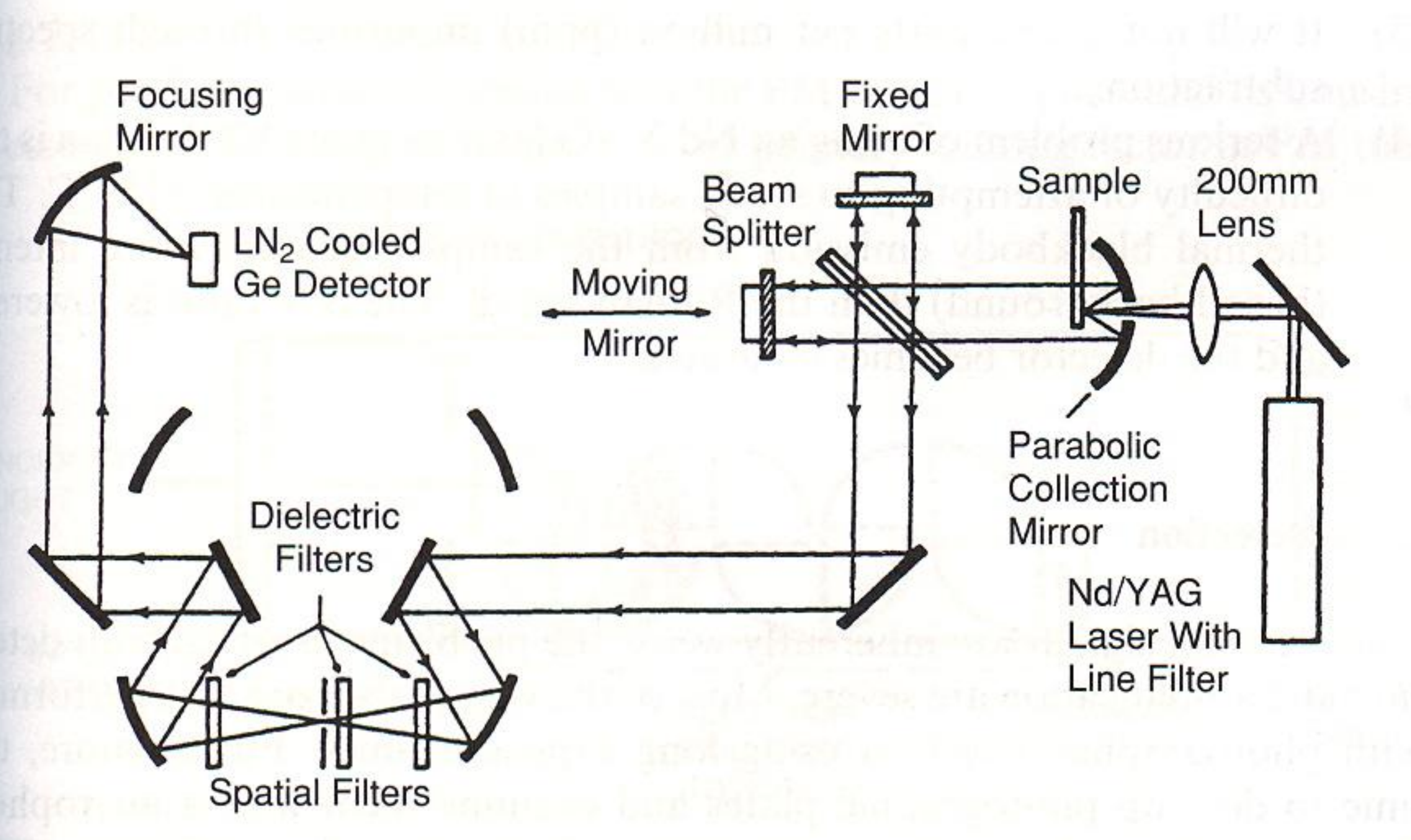

1λ, Zero path difference

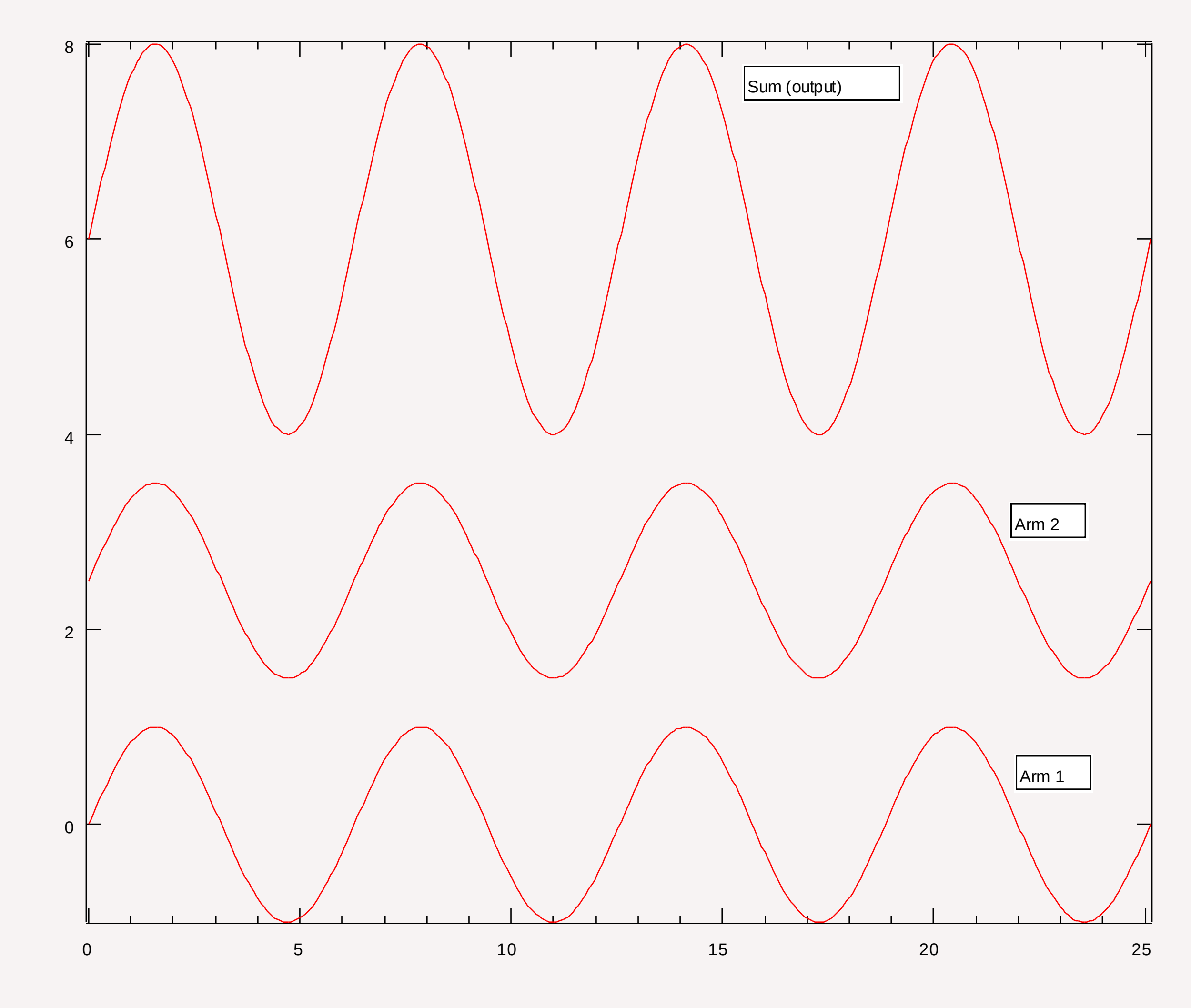

If there is a zero path difference (ZPD) between the two arms of the interferometer, then the waves will recombine and add constructively. The detector will then see a modulated, bright beam coming out of the interferometer.

Note that we are only considering one scattered wavelength!

1λ, Single interferogram

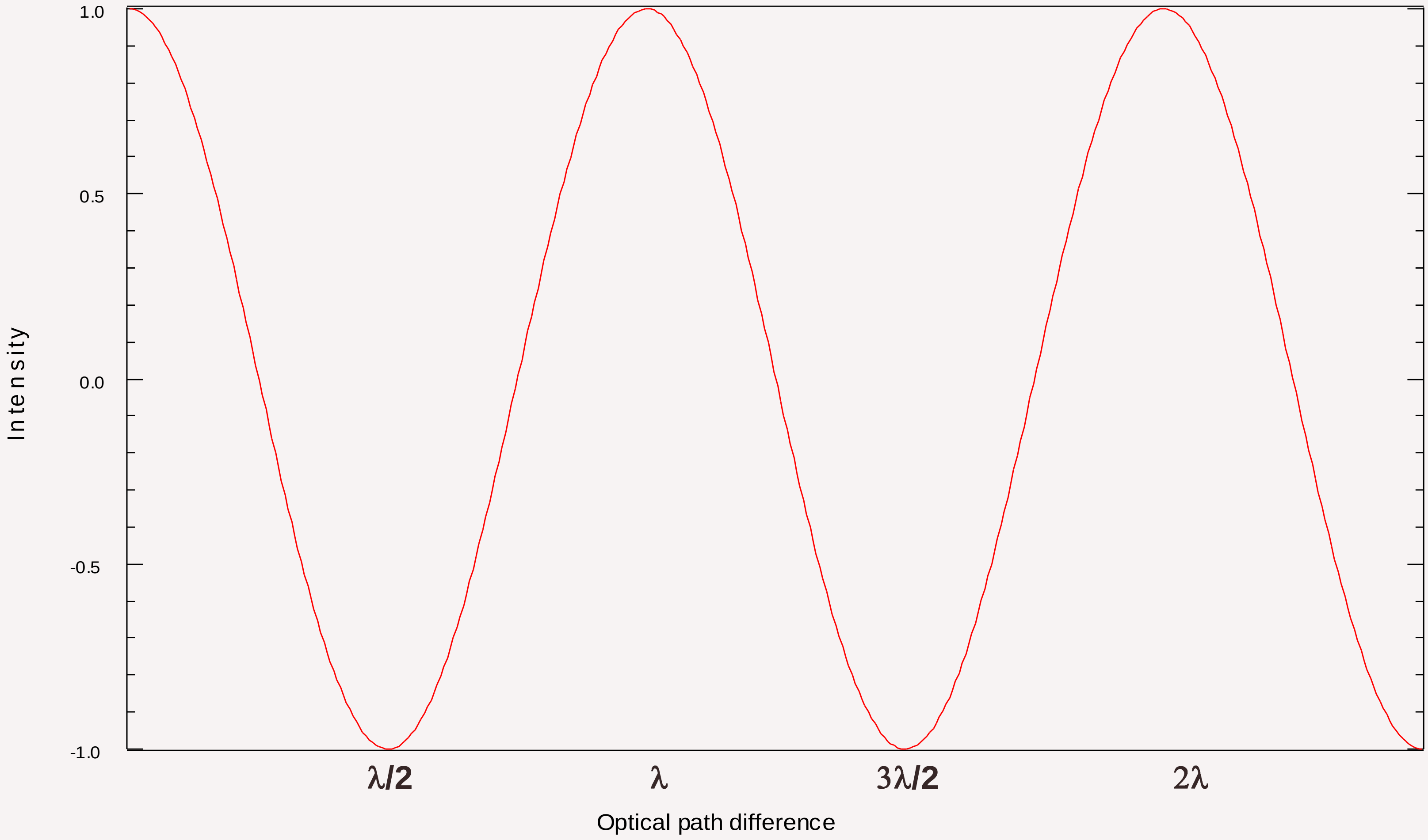

2λ, Sum of interferograms

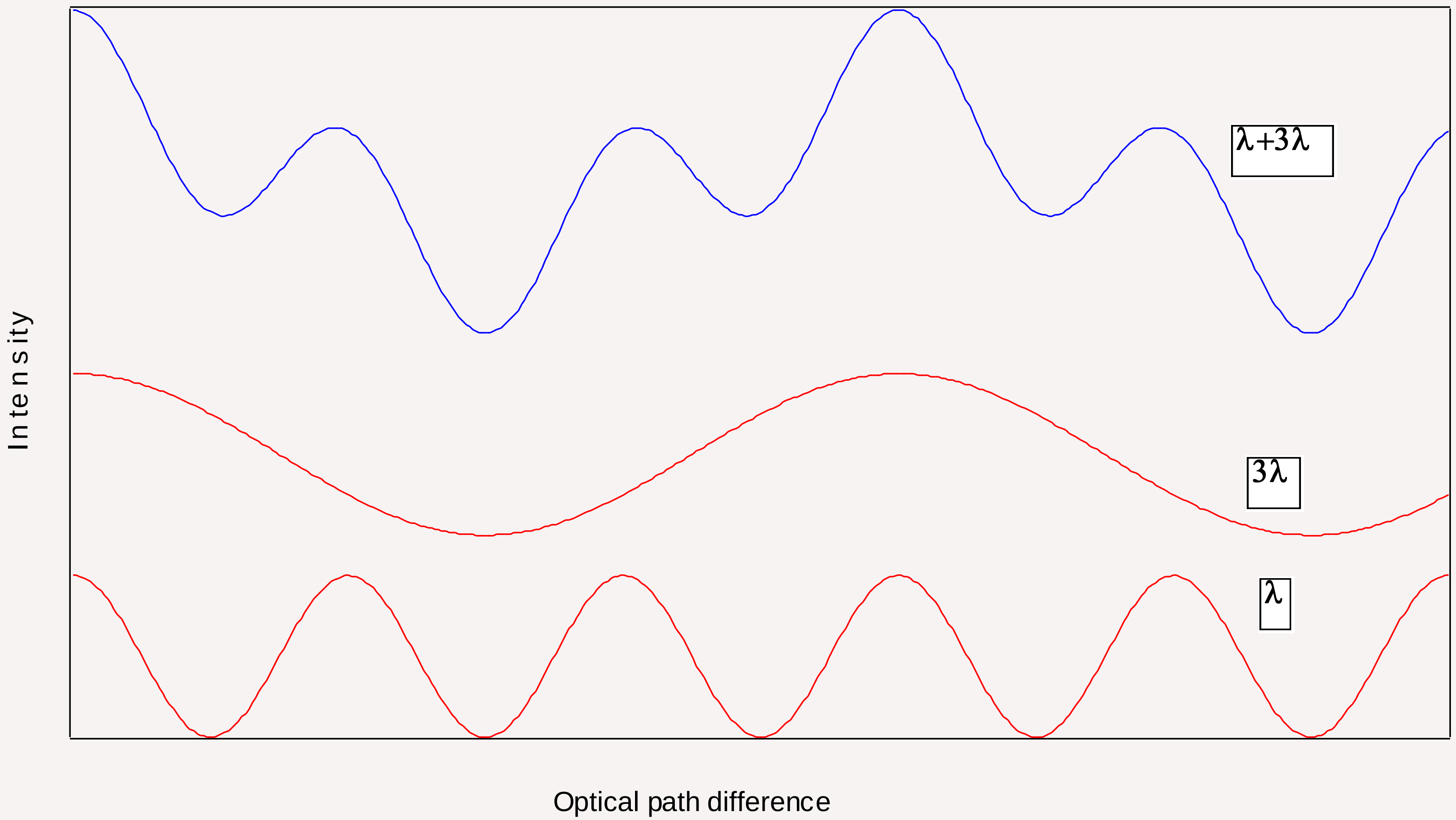

EXERCISE

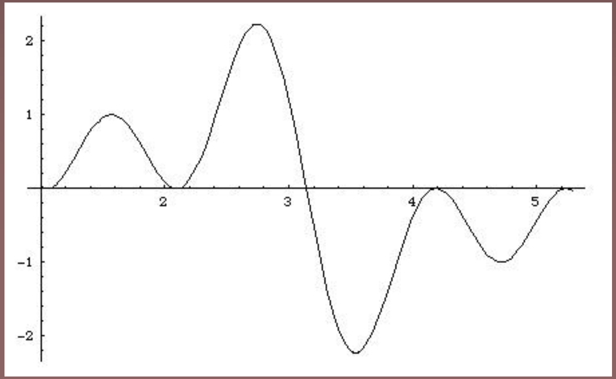

Sin(x) + Sin(3x) + Sin(5x)

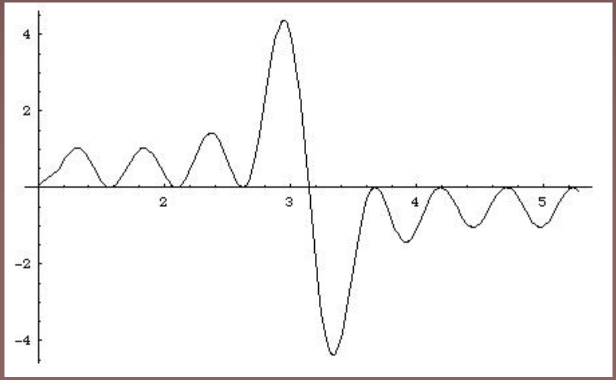

Sin(x) + Sin(3x) + Sin(5x) + Sin(7x) +Sin(9x) + Sin(11x)

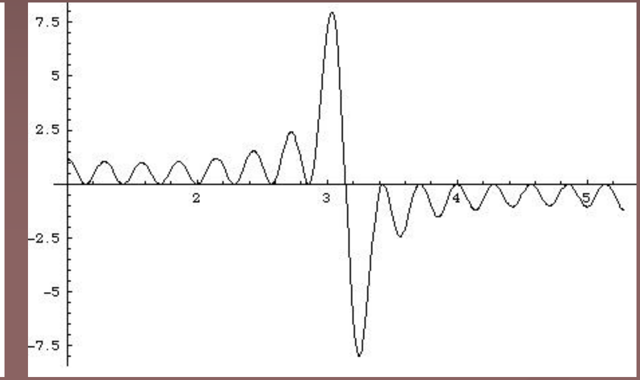

Sin(x) + Sin(3x) + Sin(5x) + Sin(7x) +Sin(9x) + …+ Sin(21x)

What would the interferogram of a large number of wavelengths look like?

EXERCISE

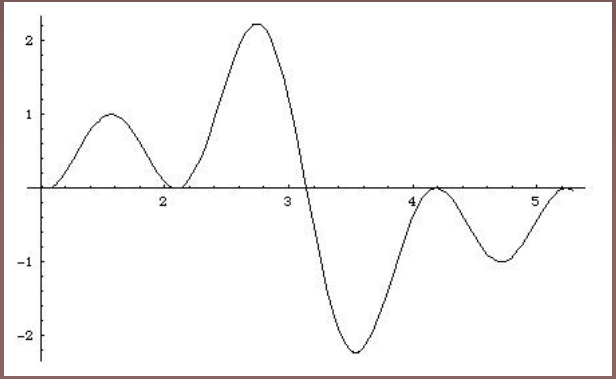

Sin(x) + Sin(3x) + Sin(5x)

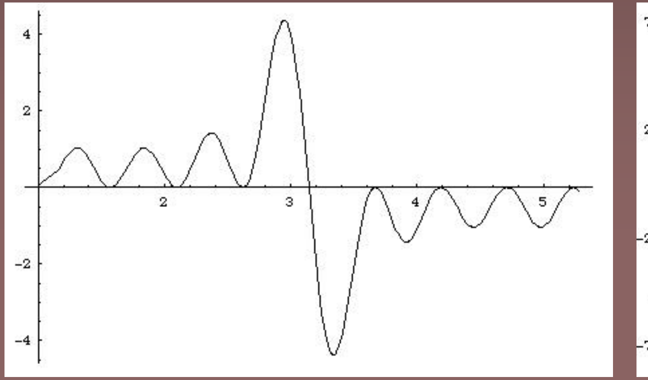

Sin(x) + Sin(3x) + Sin(5x) + Sin(7x) +Sin(9x) + Sin(11x)

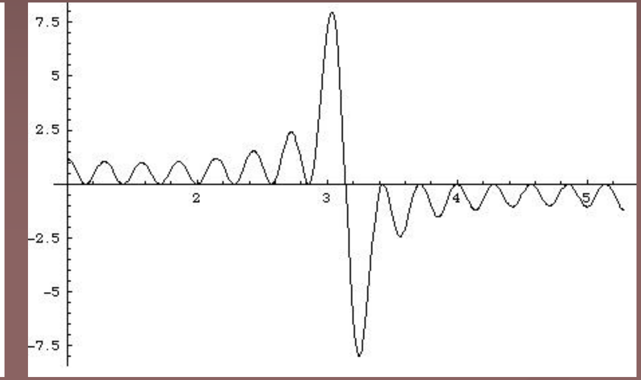

Sin(x) + Sin(3x) + Sin(5x) + Sin(7x) +Sin(9x) + …+ Sin(21x)

What would the interferogram of a large number of wavelengths look like?

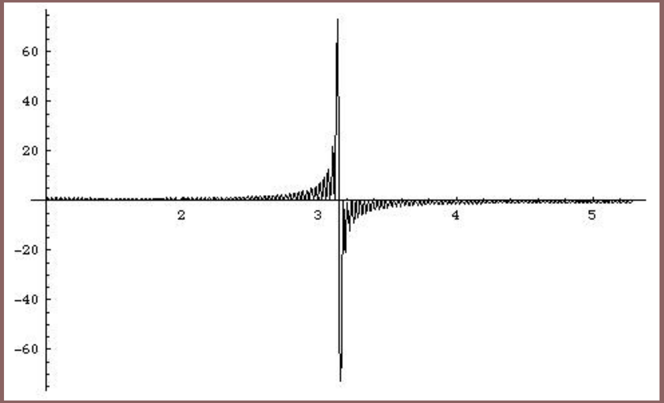

<--Calculated for first 100 odd sine terms

From FTIR-->

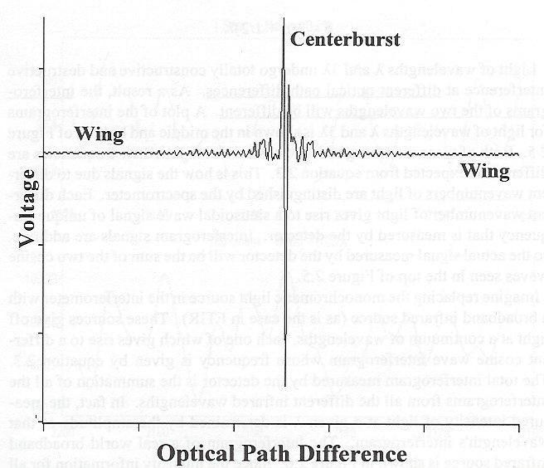

Raman microscopes

Microscope schematic

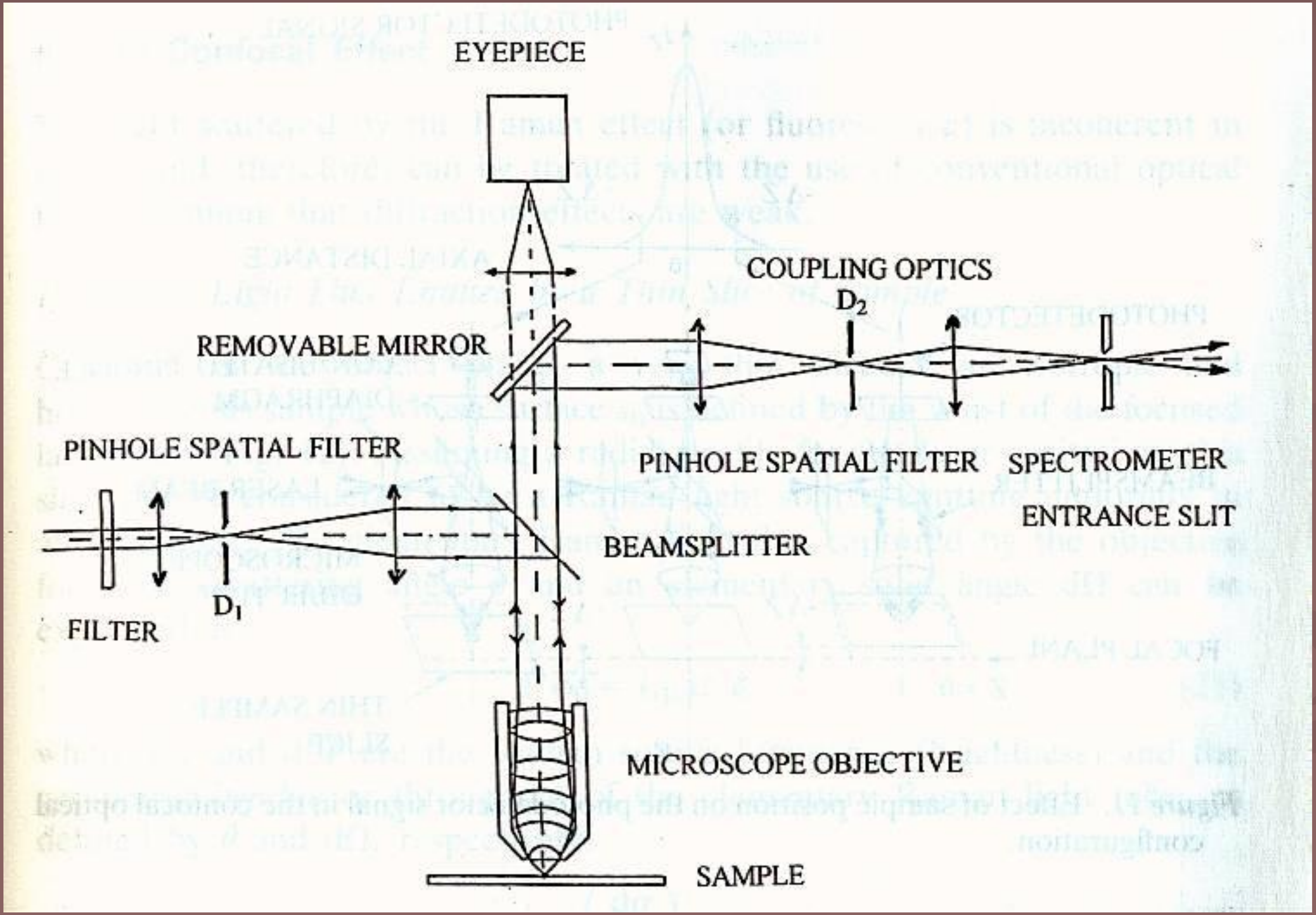

Conventional *vs.* Confocal

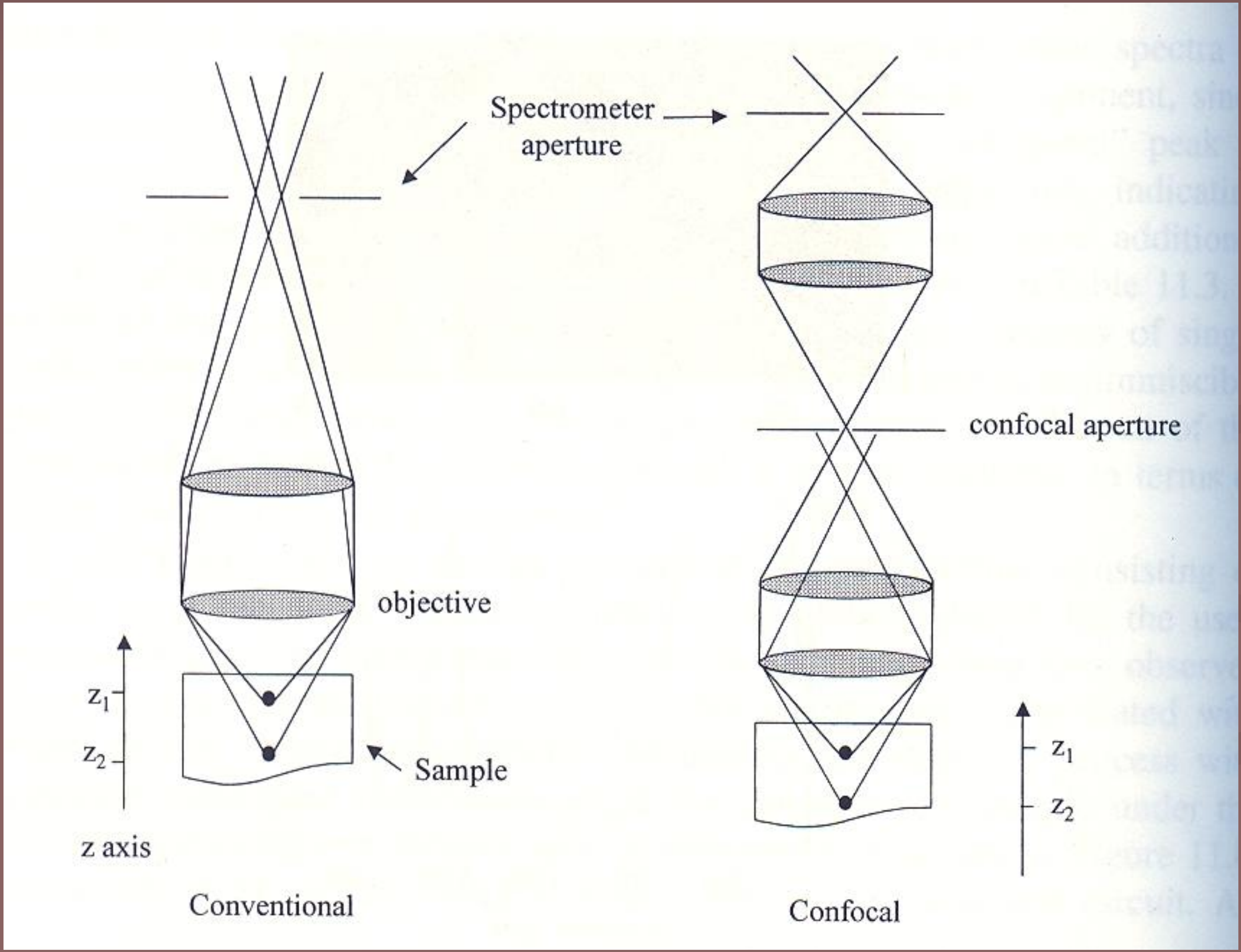

Raman microscopy

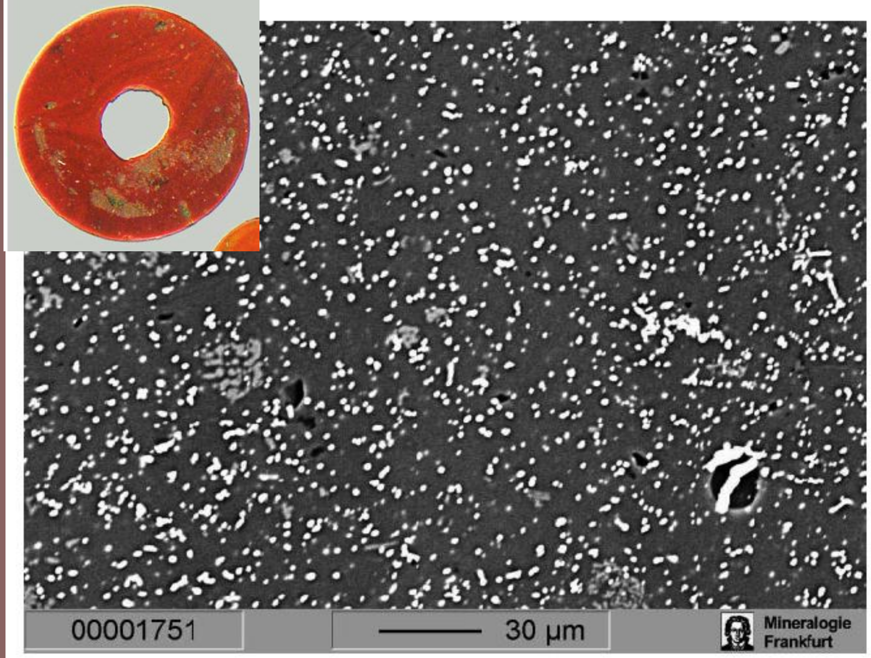

Figure 4. Small cuprite crystals of micrometre size interspersed in the glass matrix of red opaque disc-shaped beads: back-scattered image.

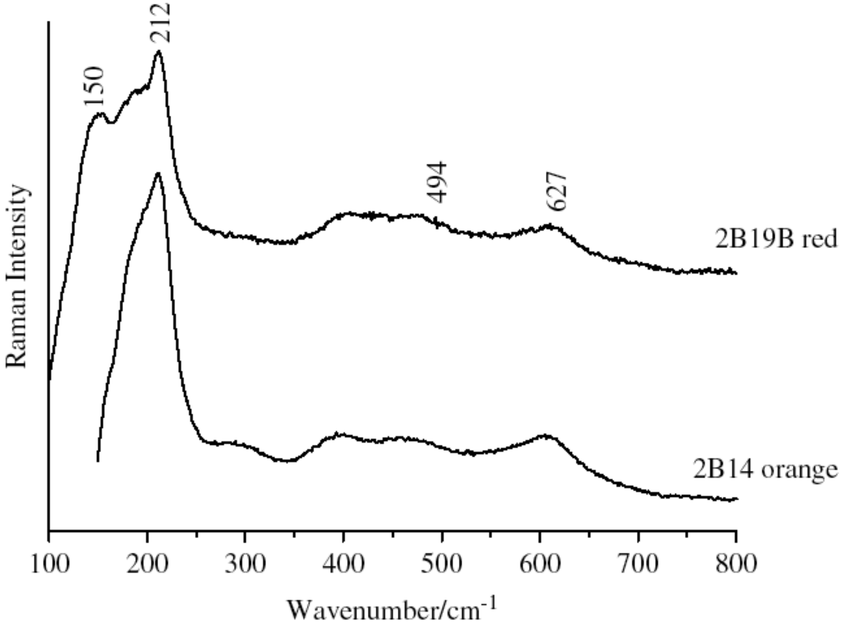

Figure 5. Raman spectra of cuprite (Cu_2O) in the red disc-shaped beads 2B19B and 2B14: excitation wavelength $\lambda = 514.5$ nm.

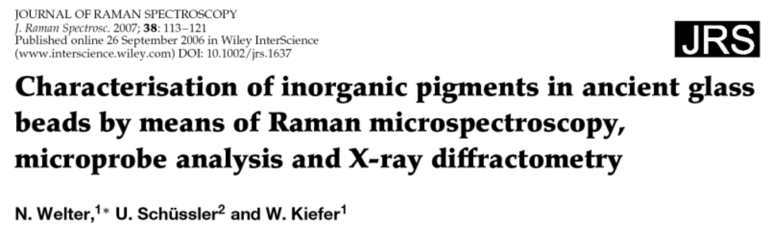

JOURNAL OF RAMAN SPECTROSCOPY
J. Raman Spectrosc. 2007; **38**: 113–121
Published online 26 September 2006 in Wiley InterScience
(www.interscience.wiley.com) DOI: 10.1002/jrs.1637

JRS

Characterisation of inorganic pigments in ancient glass beads by means of Raman microspectroscopy, microprobe analysis and X-ray diffractometry

N. Welter,[1]* U. Schüssler[2] and W. Kiefer[1]

7. References

- Raman Microscopy: Developments and Applications, G. Turrell, J. Corset, eds. (Elsevier Academic Press, 1996)
- Introductory Raman Spectroscopy, J.R. Ferraro, K. Nakamoto, C.W. Brown, Academic Press, 2003.
- Raman Spectroscopy for Chemical Analysis, R.L. McCreery (Wiley Interscience, 2000).
- Handbook of Raman Spectroscopy, I.R. Lewis, H.G.M. Edwards, eds. (Marcel Dekker, 2001)
- “Gemstone identification using Raman spectroscopy”, A.L. Jenkins, R.A. Larsen, *Spectroscopy* **19** (4), April 2004, 20 ff.
- Raman Technology for Today’s Spectroscopists, 2004 Technology primer, Supplement to Spectroscopy magazine.
- Website of J. Yvon.

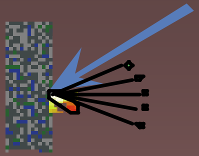

7. References

- **An Introduction to Raman Spectroscopy: Introduction and Basic Principles, by J. Javier Laserna, at** www.spectroscopynow.com/coi/cda/landing.cda?chId=6&type=Education
- Kamitsos, E. I., Y. D. Yiannopoulos, et al. (1996). "Raman and Infrared Investigation of xRb2O-(1-x)GeO2 Glasses." *J. Phys. Chem*. **100**: 11755-11765.
- Veres, M., Fule, M., Toth, S., Koos, M. Pocsik, I. (2004). “Surface Enhanced Raman Scattering (SERS) Investigations of Amorphous Carbon”, *Diam. and Rel. Mater*. **13**, 1412-1415.